Post-earthquake continuous dynamic monitoring of the *Gabbia Tower* in Mantua, Italy

Antonella Saisi [a,1], Carmelo Gentile [a,*], Marco Guidobaldi [b,2]

[a] *Politecnico di Milano, Department of Architecture, Built environment and Construction engineering (ABC), Milan, Italy*
[b] *Politecnico di Milano, Milan, Italy*

Received 28 October 2014
Received in revised form 2 February 2015
Accepted 12 February 2015

1. Introduction

Ambient vibration testing (AVT) and continuous monitoring of the structural response under ambient excitation are well-known non-destructive methodologies, generally aimed at identifying the dynamic characteristics of a structure from output-only records using operational modal analysis (OMA) techniques (see e.g. [1]).

Although AVT has become the primary modal testing method of civil engineering structures, its application to historic structures is still quite limited [2–16]. On the other hand, AVT and Structural Health Monitoring (SHM) using OMA are especially suitable to Cultural Heritage structures because of the fully non destructive and sustainable way of testing, that is performed by just measuring the dynamic response under ambient excitation and does not involve additional loads rather than those associated to normal operational conditions. It is indeed true that the response of his-toric buildings to ambient excitation is generally low (because the historical urban centers are often closed to road traffic) but this cannot be considered a prohibitive issue as highly sensitive and relatively inexpensive accelerometers are currently available on the market.

AVTs have been performed more frequently to investigate the dynamic behavior of ancient masonry towers [3–5,8,9,11–14,16] as these very common Cultural Heritage structures, that are usually slender and subjected to significant dead loads, might exhibit

* Corresponding author. Tel.: +39 (0)2 23994242; fax: +39 (0)2 23994220.
E-mail addresses: antonella.saisi@polimi.it (A. Saisi), carmelo.gentile@polimi.it (C. Gentile), marco.guidobaldi@polimi.it (M. Guidobaldi).

[1] Tel.: +39 (0)2 23994386; fax: +39 (0)2 23994220.
[2] Tel.: +39 (0)2 23994267; fax: +39 (0)2 23994220.

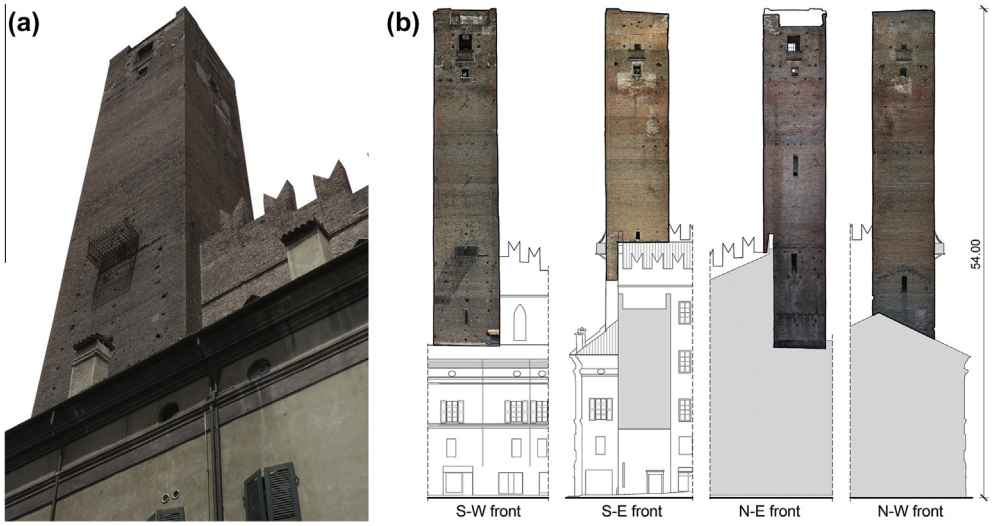

Fig. 1. (a) South-West view of the *Gabbia Tower*; (b) fronts of the tower (dimensions in m).

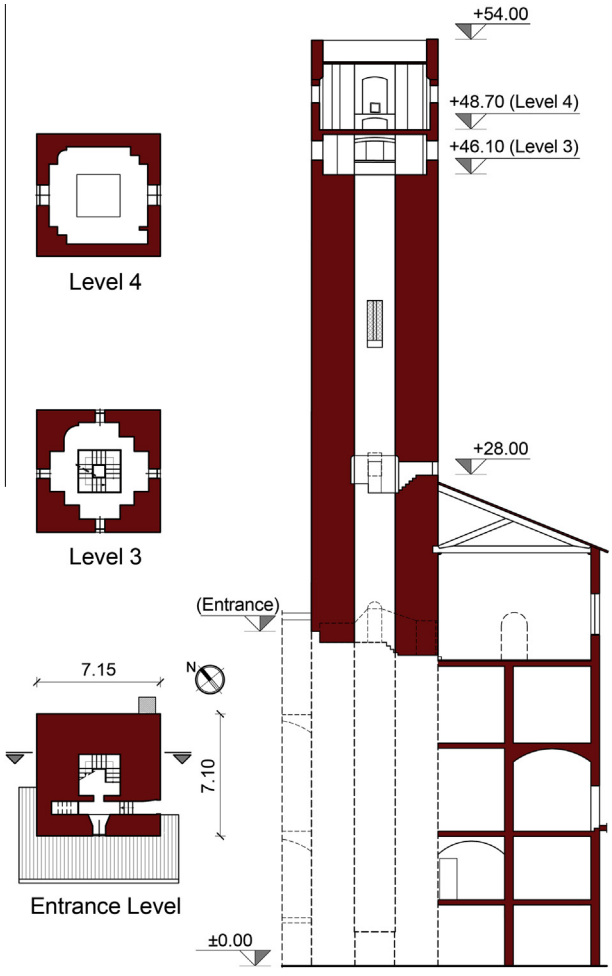

Fig. 2. Section of the tower (dimensions in m).

high sensitivity to dynamic actions, such as traffic-induced microtremors, swinging of bells [4,12,14], wind and earthquakes. In addition, the cantilever-like behavior of towers suggests the use of simple dynamic monitoring systems, consisting of few sensors installed in the upper part of the structure, with preventive conservation and/or SHM purposes [9,13,14].

The paper presents the results of a continuous dynamic monitoring program carried out on the historic *Gabbia Tower* in Mantua, Italy [17]. This project follows an extensive diagnostic investigation [18] carried out, between July and November 2012, to assess the state of preservation of the tower after the Italian seismic events of May 2012. The diagnostic procedures included detailed visual inspection and geometric survey, single and double flat jack tests, pulse sonic tests, laboratory tests on sampled mate-rials and preliminary AVTs.

The results of the post-earthquake investigation [18] highlighted the poor structural condition and the high vulnerability of the upper part of the tower, pointing out the need for structural interventions to be carried out. Furthermore, it was decided to install a simple dynamic monitoring system in the tower, as a part of the health monitoring process helping the preservation of the historic building. The instrumentation installed inside the tower consists of a 4-channel data acquisition board, with 3 piezoelectric accelerometers and 1 temperature sensor. A binary file, containing 3 acceleration time series (sampled at 200 Hz) and the temperature data, is created every hour, stored in an industrial PC on site and transmitted to Politecnico di Milano for being processed.

The main objectives of the continuous dynamic monitoring are: (a) evaluating the dynamic response of the tower to the expected sequence of far-field earthquakes; (b) evaluating the effects of temperature on the natural frequencies of the building [9,13,14]; (c) detecting any possible anomaly or change in the structural behavior. Furthermore, another possible long-term goal is evaluating the effects of the future strengthening intervention.

After a brief description of the investigated tower and the results of the post-earthquake assessment, full details are given in the paper on the monitoring system, the methodologies used to process the collected data, the effects of farfield earthquakes and the results of the continuous dynamic monitoring for a period of 8 months.

2. The Gabbia Tower in Mantua, Italy

2.1. Description of the tower and historic background

The *Gabbia Tower* (Figs. 1 and 2) [17], about 54.0 m high, is the tallest tower in Mantua and is named after the hanged dock built in the XVI century on the S-W front and originally used as open-air jail.

Fig. 3. (a) Probable merlons embedded in the masonry texture; (b) change of the surface workmanship at about 8.0 m from the top.

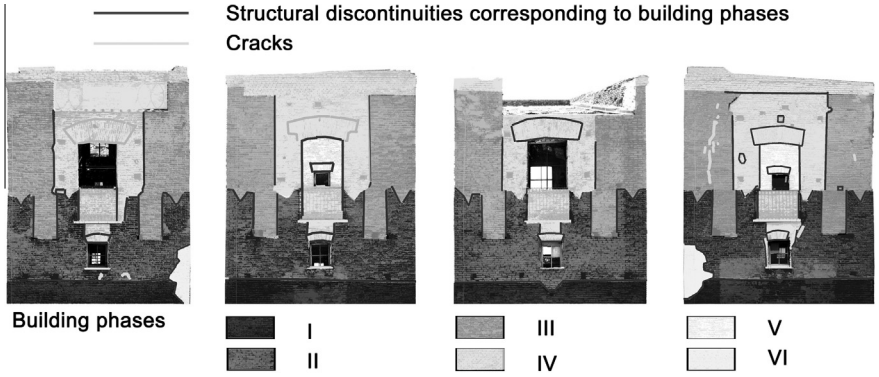

Fig. 4. Structural discontinuities detected in the upper part of the tower and supposed building phases.

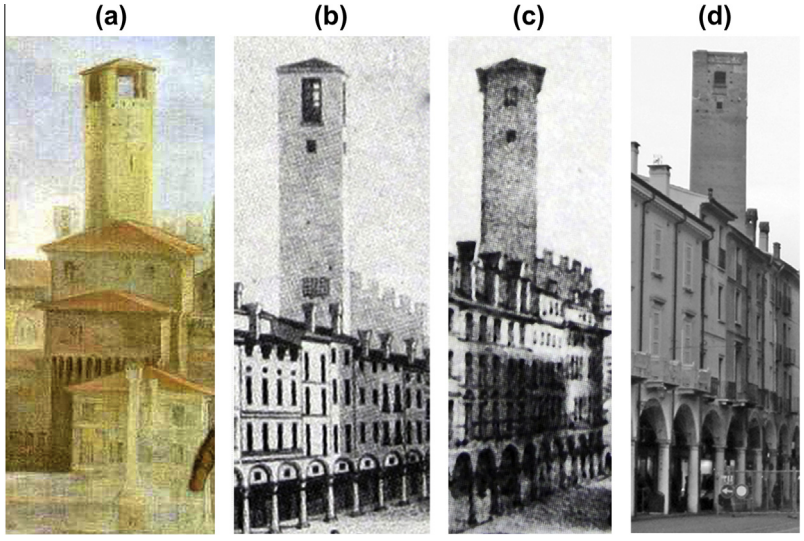

Fig. 5. Views of the *Gabbia Tower* dating back to: (a) XVII century; (b) 1830; (c) 1852 and (d) present days.

Although few historic documents are available on the tower and its evolution [17], some recent research dates the beginning of construction to the late XII century and assumes that the building was probably concluded in 1227. The tower was part of the defensive system of the Bonacolsi family, governing Mantua at the time. According to the past tradition of defensive structures, the

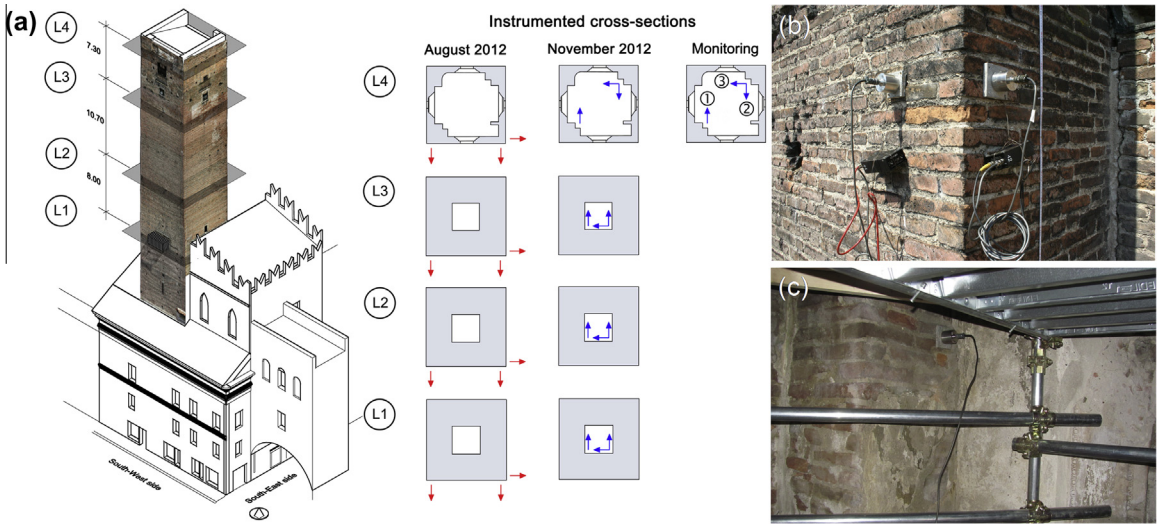

Fig. 6. (a) Instrumented cross-sections and layout of accelerometers during the preliminary tests and the continuous dynamic monitoring. Typical mounting of sensors in: (b) Summer 2012 and (c) November 2012.

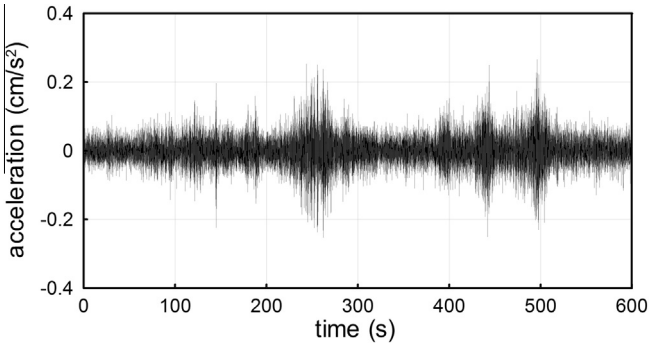

Fig. 7. Typical acceleration recorded in Summer 2012 at the top of the tower.

entrance is not located at the ground level but at a higher position (Fig. 2).

As it can be observed in Fig. 1, during the centuries a palace evolved around the tower, complicating the geometry of the structure and the mutual links between the walls. In general, the load bearing walls of the palace seem to be not effectively linked but just drawn to the tower's masonry walls, whereas the tower direct-ly supports several floors and vaults.

The tower, built in solid brick masonry, has almost square plan and the load-bearing walls are about 2.4 m thick until the upper levels, hosting a two level lodge (Fig. 2), where the masonry section decreases to about 0.7 m. During the XIX century and at the beginning of the XX century, the lodge hosted an observation and telegraph post, used for military and communication purposes. In the past, a wooden staircase was used to reach the lodge but it has not been practicable since the 90's due to lack of maintenance. The inner access to the tower was re-established in October 2012 through provisional scaffoldings in order to allow visual inspection and geometric survey of the inner load-bearing walls.

No extensive information is available on the tower past interventions but the stratigraphic survey and the masonry texture reveal passing-through discontinuities in the upper part of the building, with those discontinuities being conceivably referable to the tower evolution phases (Figs. 3–5). Traces of past structures on all fronts, the presence of merlon-shaped discontinuities (Figs. 3a and 4) and the available historic pictures (Fig. 5) indicate modifications and successive adding in the upper part of the tower. Moreover, at about 8.0 m from the top, a clear change of the brick surface workmanship (the bricks of the lower part are superficially scratched, Fig. 3b) suggests a first addition; in the same region concentrated changes of the masonry texture reveal local repair.

A first hypothesis, based on the surface discontinuity survey, could recognize the main building phases partially illustrated in Fig. 4 and difficult to date: (i) erection of the main building until the height of 46 m (probably concluded in 1227); (ii) subsequent addition until the merlon level; (iii) adding of 4 corner piers supporting a four side roof; (iv–v) opening infilling and construction of windows, crowning and new roof; (vi) repair of the South corner.

2.2. Visual inspection and on site tests

On-site survey of all outer fronts of the tower was performed between 30/07/2012 and 02/08/2012, using a movable platform. Survey of the inner load-bearing walls and local tests were carried out subsequently (November 2012), once the inner access was re-established.

The visual inspection [18] highlighted two different structural conditions, that are associated to: (a) the main part of the building, until the height of about 46 m from the ground level and (b) the upper region of the tower (Fig. 4).

No evident structural damage was observed in the lower part of the structure, where superficial decay of the materials was mainly detected. After the installation of provisional scaffoldings, pulse sonic tests and flat-jack tests were performed and confirmed the compactness of the masonry in the lower portion of the tower. Results from pulse sonic tests provided the evidence of solid brick section, with sonic velocity values ranging between 1100 m/s and 1600 m/s. Double flat jack tests were carried out: (1) on the outer S-W wall, at the ground level and (2) on the inner S–W wall (from scaffolding), at about 32.8 m from the ground level. The Young's modulus obtained from both tests turned out to be larger than 3.00 GPa. Similar information on the good quality of masonry materials results from the laboratory tests on sampled bricks and mortars.

On the contrary, the upper part of the tower (i.e. the top region, about 8.0 m high) is characterized by extensive masonry decay and the presence of several discontinuities (Fig. 4) due to the evolution of the building (Fig. 5). The poor state of preservation of this region,

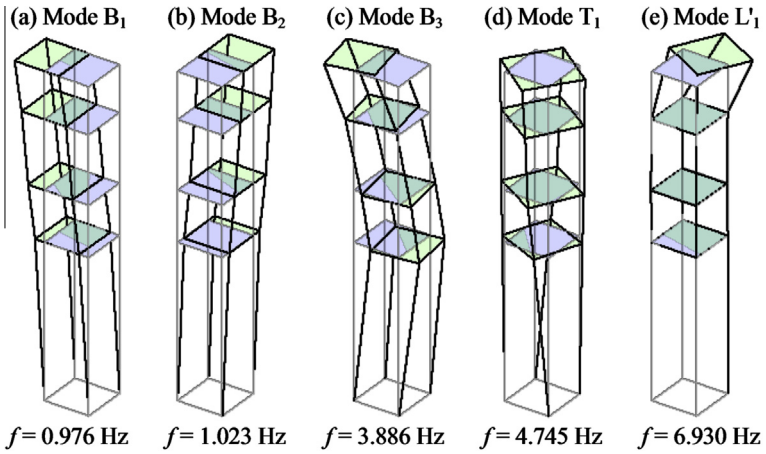

Fig. 8. Vibration modes generally identified in the first test (SSI-Data, 31/07/2012, 22:00-23:00).

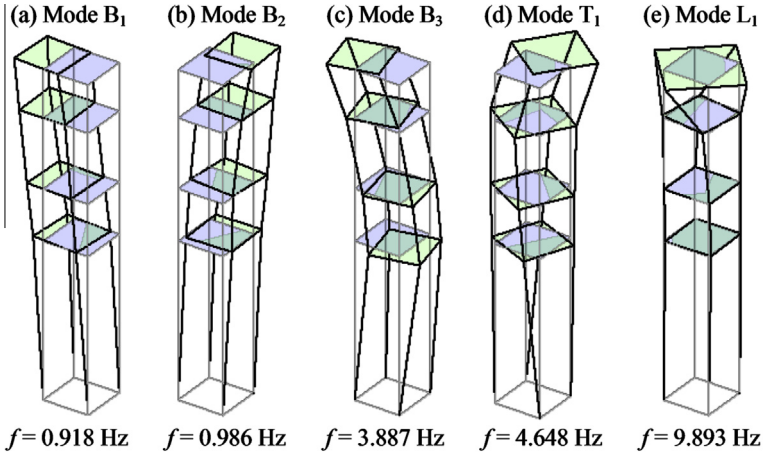

Fig. 9. Vibration modes identified (SSI-Data) on 27/11/2012.

exhibiting lack of connection or local detachment of the construction phases, was confirmed by [18]: (a) the low average value of the sonic velocity (600 m/s) obtained from pulse sonic tests; (b) the presence of one local vibration mode, involving the upper part of the tower, that was clearly identified from the response data collected for more than 24 h on the building.

It is further noticed that a wooden roof was installed in the upper part of the tower when the inner access was re-established through provisional scaffoldings. This roof, although very light, is slightly inclined in the N–E/S–W direction (as schematically shown in Fig. 6a) and directly supported by the weakest structural part of the building. It is worth underlining that the roof slope, the redundant connection with the masonry walls and the thermal effects might induce not negligible thrusts on structural walls, that are very vulnerable due to the extensive decay, the presence of several discontinuities and the lack of connection of the different adding.

3. Preliminary ambient vibration tests

3.1. Testing procedures and modal identification

Two AVTs were conducted on the tower: between 31/07/2012 and 02/08/2012, and on 27/11/2012. In the first test, since the access to the inner walls of the tower was not available, the accelerometers were mounted on the outer walls (Fig. 6a and b) making use of the movable platform employed in the same days for visual inspection. On the contrary, inner mounting of the sensors (Fig. 6a and c) was preferred in the second test, performed after the installation of metallic scaffoldings and wooden roof inside the tower. Indeed, the second test was carried out mainly to check the possible effects of those additions on the dynamic characteristics of the structure, before installing a dynamic monitoring system.

High sensitivity piezoelectric accelerometers (WR model 731A, Fig. 6b and c) were selected to measure the response of the tower. A short cable (1 m) connected each sensor to a power unit/ampli-fier (WR model P31), providing the constant current needed to power the accelerometer's internal amplifier, signal amplification and selective filtering. Two-conductor cables connected the ampli-fiers to a 24-channel data acquisition system (24-bit resolution, 102 dB dynamic range and anti-aliasing filters).

In both AVTs, the response of the tower was measured simultaneously in 12 points, belonging to the same pre-selected cross-sections along the height of the building. The sensor layouts adopted in the two tests are shown in Fig. 6a.

In the first test, acceleration data were acquired for 28 h: between 16:00 and 23:00 of 31/07/2012 and from 9:00 of 01/08/2012 to 6:00 of 02/08/2012. A typical acceleration time series, acquired in 10 min period at the upper instrumented level, is presented in Fig. 7 and highlights that a low level of ambient excitation existed during the tests, with the maximum recorded acceleration being lower than 0.4 cm/s^2. The amplitude of responses was very similar in the second test, as well.

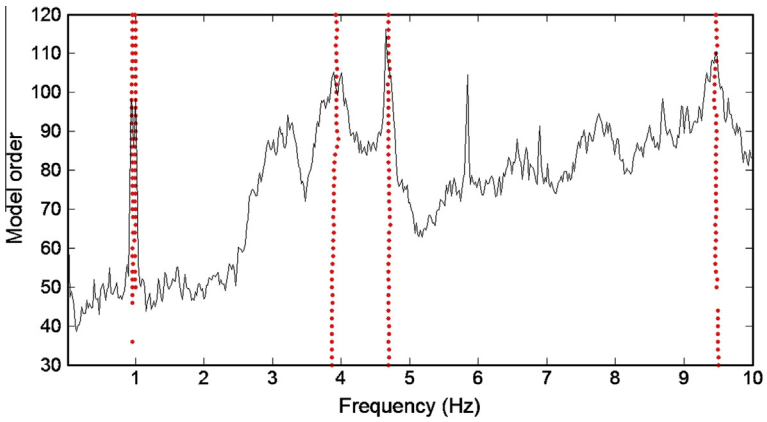

Fig. 10. Typical stabilization diagram obtained by applying the automated SSI-Cov technique to 1-h dataset.

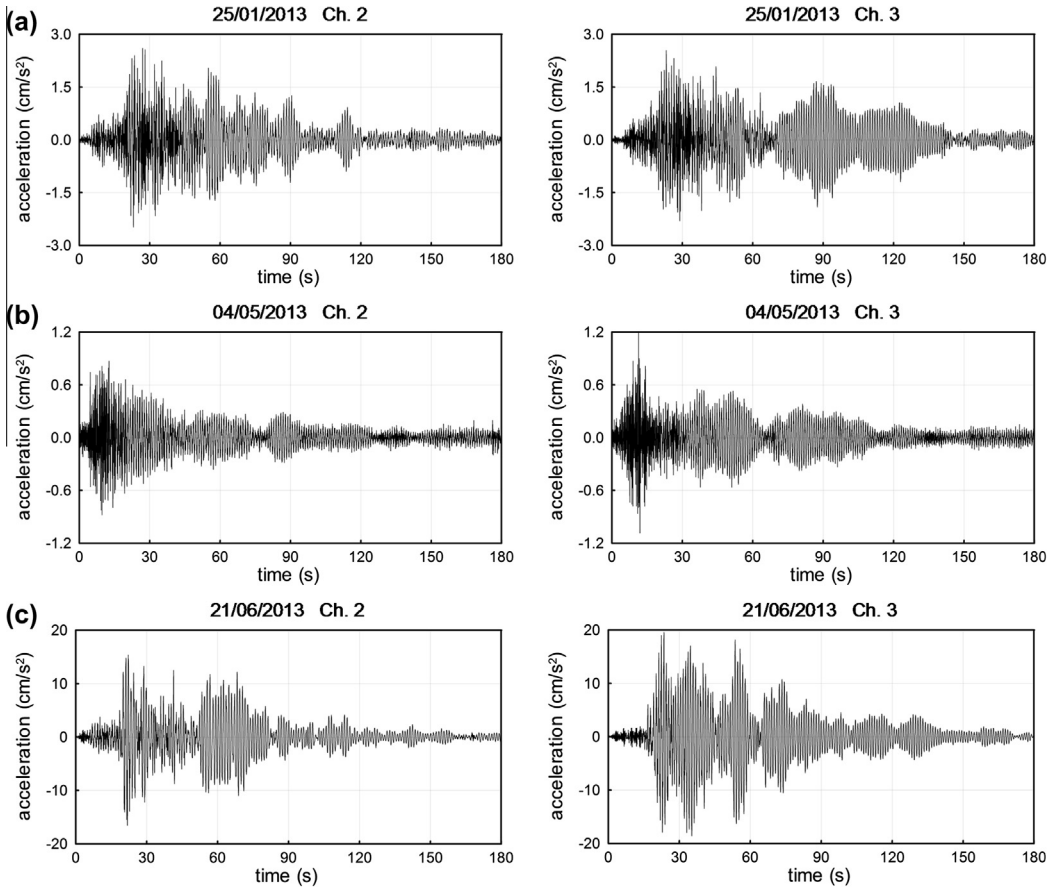

Fig. 11. Seismic responses recorded on: (a) 25/01/2013; (b) 04/05/2013 and (c) 21/06/2013.

During the first AVT, a second acquisition system was used to measure the temperature in three different points of the tower: on the S–W load-bearing wall, both indoor and outdoor temperature were measured, whereas only the outdoor temperature was recorded on the S–E front. It is worth mentioning that the changes of outdoor temperature were very significant, ranging between 25 °C and 55 °C, whereas slight variations were measured by the indoor sensor (29–30 °C), due to the high thermal inertia of the masonry walls.

During the second test, about two hours of data were collected, with the outdoor temperature being almost constant (10–11 °C).

The modal identification was performed using time windows of 3600 s and applying the data-driven Stochastic Subspace Identification technique (SSI-Data) [19,20] available in the commercial software ARTeMIS [21].

3.2. Dynamic characteristics of the tower

Notwithstanding the very low level of ambient excitation (Fig. 7) that characterized the tests, the application of the SSI-Data technique to all data sets generally allowed to identify 5 vibration modes.

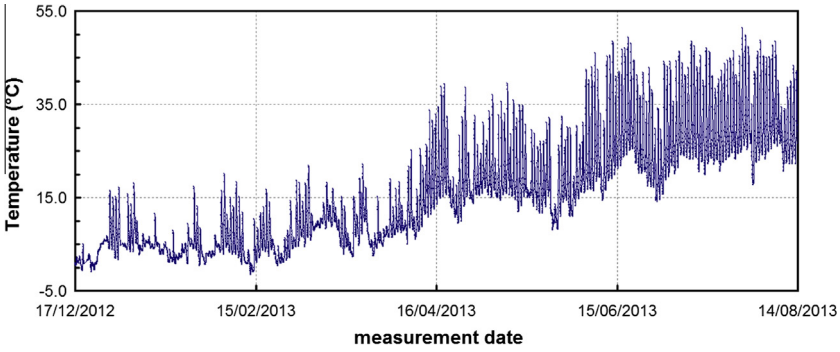

Fig. 12. Temperature variation between 17/12/2012 and 13/08/2013.

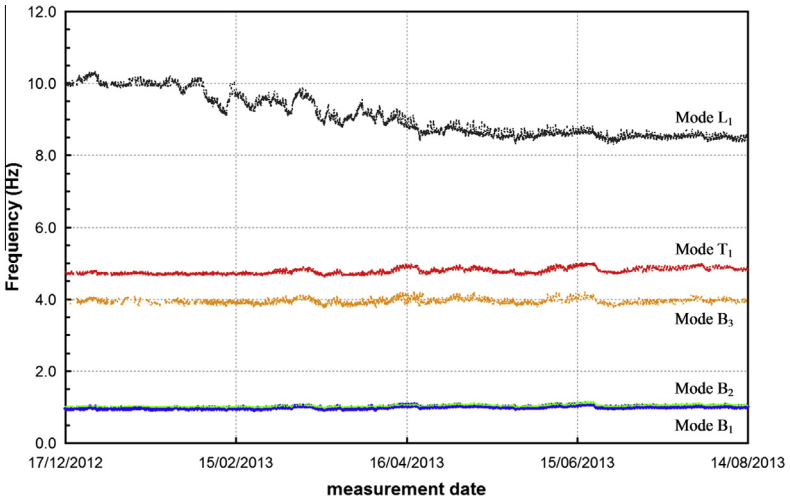

Fig. 13. Variation of identified natural frequencies between 17/12/2012 and 13/08/2013.

Table 1
Statistics of the natural frequencies identified (SSI-Cov) from 17/12/2012 to 13/08/2013.

Mode	f_{ave} (Hz)	σ_f (Hz)	f_{min} (Hz)	f_{max} (Hz)
1 (B_1)	0.989	0.035	0.910	1.102
2 (B_2)	1.029	0.031	0.961	1.148
3 (B_3)	3.940	0.073	3.758	4.194
4 (T_1)	4.768	0.082	4.621	5.010
5 (L_1)	9.076	0.573	8.298	10.327

B = bending mode; T = torsion mode; L = local mode.

Typical results of the first test, in terms of natural frequencies and mode shapes, are shown in Fig. 8, whereas Fig. 9 shows the dynamic characteristics identified in the second test. The inspection of Figs. 8 and 9 allows the following comments:

(1) Two closely spaced modes were identified around 1.0 Hz. These modes (Figs. 8a, b and 9a and b) are dominant bending (B) and involve flexure in the two main planes of the tower, respectively.
(2) The third mode (Figs. 8c and 9c) involves dominant bending in the N–E/S–W plane with slight components also in the orthogonal N–W/S–E plane.
(3) Beyond the difference in terms of natural frequency (that are related to the effects of changing temperature, as it will be shown in Section 5), the mode shapes of bending modes B_1–B_3 did not exhibit significant changes (see Figs. 8a–c and 9a–c). Hence, the metallic scaffolding and the wooden roof practically do not affect those modes.
(4) The upper modes identified in the first test involved torsion (T) of the entire structure (Fig. 8d) and coupled torsion-bending of the upper portion of the tower (Fig. 8e), respectively. The presence of the local vibration mode L_1' (Fig. 8e) provided further evidence of the structural effect of the change in the masonry quality and morphology observed on top of the tower during the visual inspection.
(5) In the second test, the fourth mode (Fig. 9d) involves dominant torsion of the tower until the height of 46 m and coupled torsion-bending of the upper level. The identified frequency did not change appreciably with respect to the first dynamic survey, but the mode shape looks significantly different. The torsion component is still dominant in the lower portion of the structure, whereas the upper part is also characterized by dominant bending. In other words, after the installation of the wooden roof, the mode T_1 (Fig. 9d) becomes a sort of superposition of previous modes T_1 (Fig. 8d, lower part of the structure) and L_1' (Fig. 8e, upper part of the structure).
(6) In the second test, the previous local mode L_1' (Fig. 8e) has been "replaced" by another local mode (denoted to as L_1 in the following), with higher frequency of 9.89 Hz and involving torsion of the upper part of the tower (Fig. 9e). This local mode, not identified before, is probably related to the increase of connection between the masonry walls of the upper part of the tower induced by the new covering.

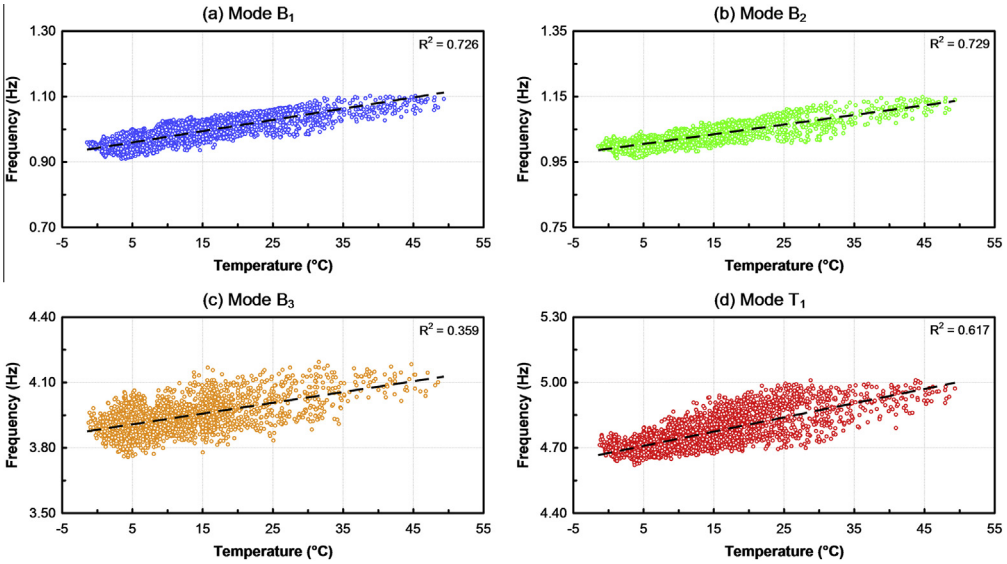

Fig. 14. Variation of identified natural frequencies (global modes) versus temperature between 17/12/2012 and 20/06/2013.

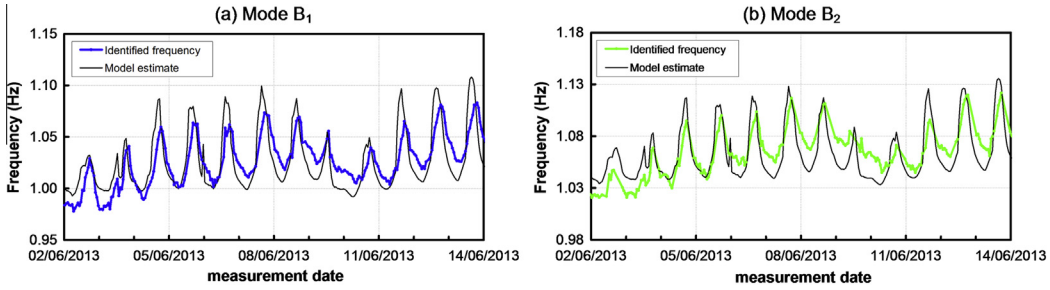

Fig. 15. Typical prediction of natural frequency obtained from linear model with temperature input only: (a) mode B_1; (b) mode B_2.

The previous comments 5–6 allow to conclude that especially the dynamic characteristics of the upper part of the building are significantly affected by the wooden roof adding. The roof, even if very light, mainly acts as a mass added in a vulnerable area, although it probably exerts also some binding effect on the dismantled masonry characterizing the upper part of the tower.

4. Description of the monitoring system and data analysis

Few weeks after the execution of the second AVT, a simple dynamic monitoring system was installed in the tower. The system is composed by:

(a) One 4-channels data acquisition system (24-bit resolution, 102 dB dynamic range and anti-aliasing filters).
(b) 3 piezoelectric accelerometers (10 V/g sensitivity, ±0.50 g peak and 0.05–500 Hz frequency range), mounted on the cross-section at the crowning level of the tower (Fig. 6a).
(c) One temperature sensor, installed on the S–W front and measuring the outdoor temperature on the wall.
(d) One industrial PC on site, for the system management and data storage.

An automatic signal acquisition toolkit was implemented in LabVIEW to record the acceleration and temperature signals and to create a binary file every hour. Each file is stored in the local PC and transmitted to Politecnico di Milano for being processed.

The continuous dynamic monitoring system has been active since late December 2012. As in the preliminary tests, modal identification was performed using time windows of 3600 s, in order to comply with the widely agreed recommendation of using an appropriate duration of the acquired time window (ranging between 1000 and 2000 times the fundamental period of the structure, see e.g. [22]) to obtain accurate estimates of the modal parameters from OMA. In fact, OMA methods assume that the excitation input is a zero mean Gaussian white noise and the longer is the acquired time window, the more closely this assump-tion is verified.

The sampling frequency was 200 Hz, which is much higher than that required for the investigated structure, as the significant frequency content of signals is below 12 Hz. Hence, low pass filtering and decimation were applied to the data before the use of the identification tools. More specifically, the acceleration time series were low-pass filtered, using a 7^{th} order Butterworth filter with cut-off frequency of 20 Hz, and decimated 5 times, reducing the sampling frequency from 200 Hz to 40 Hz.

The data files received from the monitoring system are managed in LabVIEW, where the following tasks are automatically performed [23]: (a) creation of a database with the original data; (b) preliminary pre-processing (i.e. de-trending, automatic recognition and extraction of possible seismic events); (c) evaluation of hourly-averaged acceleration amplitudes and temperature; (d) low-pass filtering and decimation of each dataset; (e) creation of a second database, with essential data records, to be used in the modal identification phase.

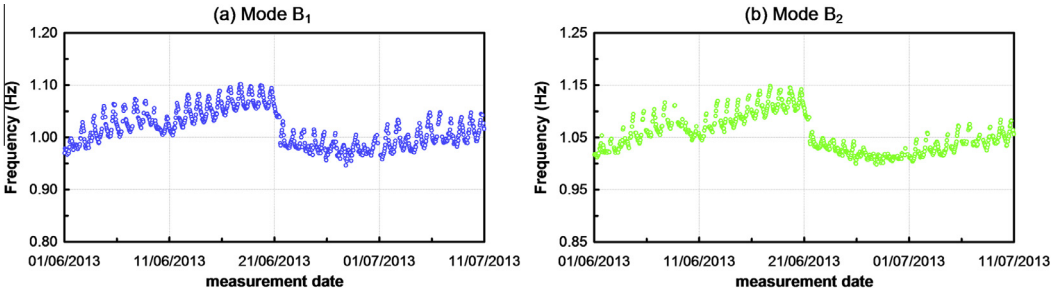

Fig. 16. Variation of natural frequency between 01/06/2013 and 10/07/2013: (a) mode B_1; (b) mode B_2.

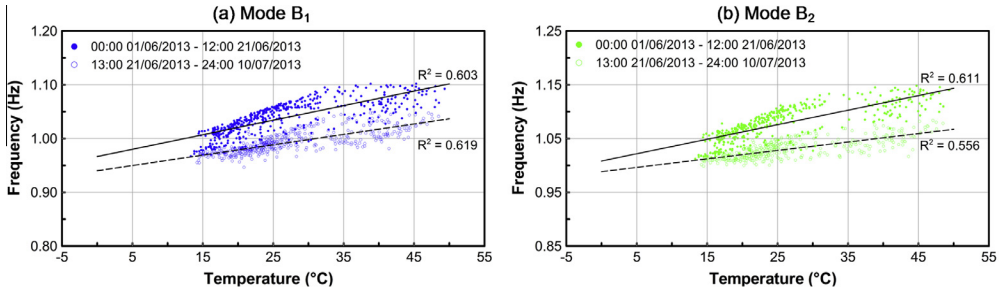

Fig. 17. Change in the frequency-temperature correlation induced by the seismic event of 21/06/2013: (a) mode B_1; (b) mode B_2.

The modal parameters of the tower are extracted from the measured acceleration data using an automated procedure [24] based on the covariance-driven Stochastic Subspace Identification (SSI-Cov) algorithm [19,20].

In the SSI-Cov algorithm, the covariance matrices of the m measured outputs are evaluated – for positive time lags varying from $1\Delta t$ to $(2i–1)\Delta t$ – to fill a $(mi \times mi)$ block Toeplitz matrix, that is decomposed to obtain stochastic subspace models of increasing order n. In the automated procedure [24], each resulting stabilization diagram (where the modes obtained with increasing model order are represented together) was firstly "cleaned" from certainly spurious modes by checking the non-physical characteristics of each point (i.e. mode) of the stabilization diagram through mode shape complexity as well as stability and range of damping ratios [25]. Similar modes in the cleaned stabilization diagram are grouped together and the modal parameters are estimated, based on the sensitivity of frequencies and mode shapes to the increase of the model order. Finally, the identified frequencies and modal deflections are compared to the reference ones estimated in the preliminary tests (Fig. 9).

In the present application, the time lag parameter i was set equal to 70 and the data was fitted using stochastic subspace models of order n varying between 30 and 120.

A typical stabilization diagram – obtained applying the automat-ed SSI-Cov algorithm [24] to a dataset recorded on 08/02/2013 – is shown in Fig. 10. The stabilization diagram is shown, after cleaning and selection of physical modes corresponding to the references, along with the first Singular Value (SV) line of the spectral matrix, which is the mode indication function adopted in the Frequency Domain Decomposition (FDD) method [26]. The inspection of Fig. 10 clearly highlights that the alignments of the stable poles in the stabilization diagram of the SSI-Cov technique provide a clear indication of the tower modes and those alignments of stable poles correspond to local maxima in the first SV line of the FDD procedure.

Between January and June 2013, the monitoring system acquired the tower's response to different earthquakes occurred in the neighboring regions. Fig. 11 shows examples of the accelerations recorded during some seismic events, with the maximum response exceeding several times the highest level of normally observed ambient vibrations (0.4–0.5 cm/s^2, Fig. 7). The acceleration times series of Fig. 11 refer to the measurement points (channels) denoted to as 2 and 3, respectively, in the schematic of the monitoring sensors illustrated in Fig. 6a. It should be noticed that the strongest seismic event (Fig. 11c, corresponding to the earthquake which hit the Garfagnana area in Tuscany on 21/06/2013) produced significant effects on the *Gabbia Tower*, as it will be discussed in Section 5.

5. Monitoring results

This section summarizes the main results of the dynamic monitoring for a period of 8 months, from 17/12/2012 to 13/08/2013. During this time period, 5760 1-h datasets were collected and automated modal identification was carried out.

Fig. 12 presents the evolution of the outdoor temperature on the S–W front during the period from 17/12/2012 to 13/08/2013 and shows that the temperature changed between −2 °C and 45 °C with significant daily variations in sunny days.

Automated identification of the modal frequencies from the datasets collected in the same period provided the frequency tracking shown in Fig. 13, whereas the corresponding statistics of natural frequencies are summarized in Table 1. This table includes the mean value (f_{ave}), the standard deviation (σ_f) and the extreme values (f_{min}, f_{max}) of each modal frequency. It should be noticed that standard deviations are larger than 0.03 Hz for all global mod-es and especially significant for the local mode, whose natural frequency varies from about 10.33 to 8.30 Hz in 8 months.

5.1. Global modes

The inspection of Figs. 12 and 13 firstly suggests that the slight fluctuation of the natural frequencies of global modes (B_1–B_3 and T_1, Figs. 9a–d) follows the temperature variation. In order to better demonstrate the effect of changing temperature on the modal

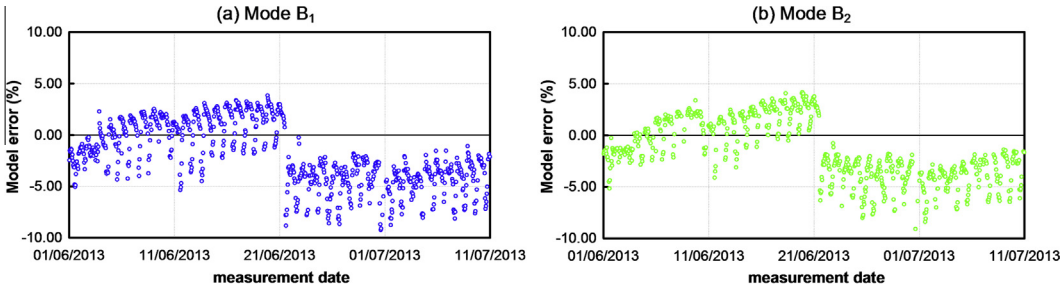

Fig. 18. Change in the prediction error induced by the seismic event of 21/06/2013: (a) mode B_1; (b) mode B_2.

frequency changes, the simplest approach is to plot each frequency with respect to temperature. Fig. 14 shows the natural frequencies of the global modes plotted with respect to temperature along with best fit lines and the coefficient of determination R^2 [27]. The plots in Fig. 14 refer to the period from 17/12/2012 to 20/06/2013 and reveal a clear dependence of the investigated natural frequencies on temperature. More specifically, the natural frequencies of the global modes exhibit an almost linear correlation with the temperature, with R^2 being larger than 0.72 for modes B_1, B_2 (Figs. 14a and b) and equal to about 0.62 for mode T_1 (Fig. 14d); the frequency–temperature correlation seems less strong for the bending mode B_3 (Fig. 14c), with R^2 being quite low (0.36) in comparison with the values of the other modes. Nevertheless, Fig. 14 confirms what already observed in the first dynamic survey [18]: the natural frequency of global modes tends to increase with increased temperature. This behavior, observed also in other long-term studies of masonry towers [9,13,14] can be explained through the closure of superficial cracks, minor masonry discontinuities or mortar gaps induced by the thermal expansion of materials. Hence, the temporary "compacting" of the materials induces a temporary increase of stiffness and modal frequencies, as well.

Fig. 14 (as well as the large values of R^2) suggests the possibility of predicting the identified natural frequency $f_i(T_k)$ of global modes B_1, B_2 and T_1 by using a simple linear model, with the measured temperature as its only input:

$$f_i(T_k) = f_i^*(T_k) + \varepsilon_{ik} = f_{i0} + \alpha_i T_k + \varepsilon_{ik} \quad (1)$$

where T_k is the measured temperature at k-th hour, f_{i0} and α_i are the coefficients of the model (determined from least square fit of data), $f_i^*(T_k) = f_{i0} + \alpha_i T_k$ is the prediction of the i-th frequency and ε_{ik} is the prediction error.

Using the frequency–temperature data reported in Fig. 14 as training data sets, the model (1) takes the form:

$$f_{B1}^*(T_k) = 0.943 + 0.0034T_k \quad (2)$$

$$f_{B2}^*(T_k) = 0.990 + 0.0030T_k \quad (3)$$

$$f_{T1}^*(T_k) = 4.676 + 0.0065T_k \quad (4)$$

for the frequency of modes B_1, B_2 and T_1, respectively. Fig. 15 shows typical estimates of the frequency change of the two lower modes.

As previously pointed out, data sets related to far-field seismic events were recorded on 25/01/2013, 04/05/2013, 19/06/2013 and 21/06/2013. The latter event, corresponding to a significant earthquake occurred in the Garfagnana region, determined acceleration responses on the top of the tower, that were more than 40 times larger (Fig. 11c) than the usual ambient vibration responses (Fig. 7).

Zooming in on the time evolution of the natural frequencies of lower modes B_1 and B_2, as shown in Fig. 16, highlights a clear drop of those modal frequencies, corresponding to the occurrence of the seismic event on 21/06/2013. The frequency shift is even more clear by inspecting the frequency content of the data recorded in the hour before and after the seismic event, respectively.

In order to investigate whether the frequency shifts are permanent or not, the frequency–temperature relationships were inspected, including data collected in the 3 weeks before and after the earthquake. The results of this check are summarized in Fig. 17, where best fit lines have been added as a visualization aid: the regression lines exhibit a remarkable variation after the seismic event, with the range of temperature variation being almost unchanged. Furthermore, Fig. 18 plots the errors of the models (2) and (3) described above for the first and second modal frequency, and highlights that the prediction errors increase and clearly depart from the previous trend after the earthquake occurrence.

Hence, the arrangement of the frequency–temperature points before and after the earthquake and the variation of the regression lines (Fig. 17) as well as the increase of the prediction errors (Fig. 18) indicate that the observed slight frequency shifts are not reversible. It is worth mentioning that this conclusion is fully confirmed by the results subsequently provided by the continuous dynamic monitoring.

Based on the previous evidence, it can be stated that the limited number of sensors installed in the structure allows the tracking of automatically identified natural frequencies and to distinguish between environmental and damage effects on the natural frequencies; on the other hand, more extensive instrumentation along the height of the tower is needed to obtain information also on the damage location and extent.

5.2. Local mode

The time evolution of the natural frequency of the upper mode, i.e. the local mode L_1 (Fig. 9e), deserves some concern because the trend of this frequency is very different from the others (Fig. 13): the modal frequency exhibits more significant fluctuations and clearly decreases in time, from an initial value of about 10.0 Hz to a final value of about 8.5 Hz at the end of the examined time period.

A careful inspection of Fig. 13 reveals that 3 clear drops of the natural frequency took place: (a) between 03/02/2013 and 04/02/2013; (b) between 14/03/2013 and 15/03/2013 and (c) between 13/04/2013 and 15/04/2013. These drops divide the analyzed time period in 4 parts, that are also easily observable by plotting the modal frequency versus the measured outdoor temperature, as shown in Fig. 19. This figure refers to the time interval from 07/01/2013 to 14/06/2013 and highlights that the clouds of temperature–frequency points, corresponding to each of the 4 different periods, are characterized by similar slope of the best fit line, whereas the average frequency value significantly decreases. More specifically, the average modal stiffness (i.e. the natural frequency) of the local mode tends to decrease as: (a) the average daily

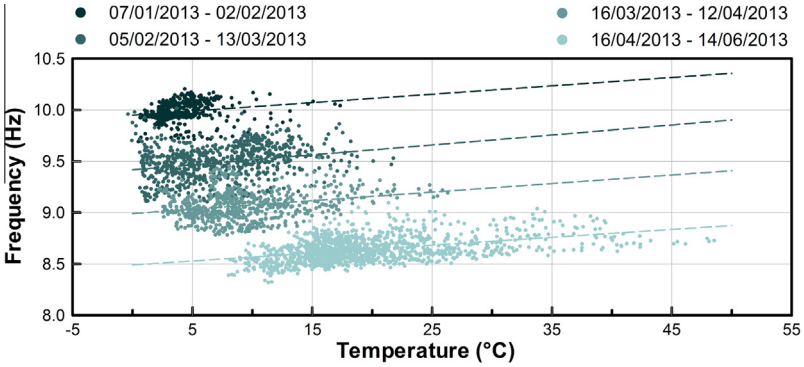

Fig. 19. Variation of natural frequency of local mode L_1 versus temperature between 07/01/2013 and 14/06/2013.

temperature increases and (b) the temperature daily range includes higher temperatures. This behavior is conceivably related to the increase of the thrust exerted by the added inclined roof on the supporting walls with increased temperature: as the thrust increases, a worsening of the connection between the masonry portions of a very heterogeneous region of the structure is induced, so that the progressive development of damage mechanisms has to be expected.

6. Conclusions

The paper focuses on the post-earthquake dynamic monitoring of the *Gabbia Tower* in Mantua, Italy.

After the seismic events of May 2012, an extensive research program has been performed to assess the state of preservation of the tower [18]. The post-earthquake investigation highlighted the poor structural condition and the high vulnerability of the upper part of the tower, characterized by the presence of several discontinuities due to the historic evolution of the building, local lack of connection and extensive masonry decay. The poor state of preservation of the same region was confirmed by the observed dynamic characteristics and one local mode, involving the upper part of the tower, was clearly identified in preliminary dynamic tests. Since the mode shapes obtained from the dynamic tests highlighted the possibility of identifying the tower vibration modes from the responses collected at the upper level, a simple dynamic monitoring system was installed in that region of the building, as a part of the health monitoring process aimed at helping the preservation of the historic structure.

Based on the time evolution of the modal frequencies automatically identified between 17/12/2012 and 13/08/2013 (8 months, 5760 datasets of 1 hour each), the following conclu-sions can be drawn:

(1) The identified natural frequencies of the tower global modes were observed to vary by 5–11%, whereas the measured temperature ranged from −2 °C to 45 °C.
(2) The temperature turned out to be a dominant driver of daily fluctuation of the frequency of global modes. More specifically, the modal frequencies increase with increased temperature and the correlation is almost linear for the lower bending and torsion modes of the tower, so that a simple linear model (with the measured temperature as its only input) should be used to predict the natural frequency of those modes.
(3) The occurrence of a far-field seismic event induced a slight decrease of the natural frequency of the fundamental modes. The evidence of this conceivably permanent damage is provided by the comparison of the modal peaks identified before and after the earthquake, and confirmed by the subsequent frequency tracking.
(4) The frequency of the local mode, involving the upper part of the tower, exhibited a complex evolution, characterized by remarkable fluctuations and significant decrease in time (about 15% in 8 months). In addition, the modal frequency tends to decrease as both the average daily temperature increases and the temperature daily range includes higher temperatures. In the authors' opinion, this abnormal behavior – increasing with increased temperature – is conceivably associated to the increase of the thrust exerted by the added wooden roof on the supporting walls and to the consequent worsening of the connection between the heterogeneous masonry portions characterizing the upper part of the tower.

Furthermore, it is worth mentioning that the information obtained from the preliminary dynamic tests as well as from the continuous monitoring might be used to validate the assumptions adopted in numerical (Finite Element) models of the tower and especially to address the uncertainties related to the interaction between the tower and the neighboring palace [5], [16] and the structural parameters characterizing the different parts of the historic building.

Acknowledgements

The investigation was supported by the Mantua Municipality. M. Antico, M. Cucchi (VibLab, Laboratory of Vibrations and Dynamic Monitoring of Structures, Politecnico di Milano) and Dr. L. Cantini are gratefully acknowledged for the assistance during the visual inspection, the field tests and the installation/maintenance of the monitoring system.

References

[1] Magalhães F, Cunha A. Explaining operational modal analysis with data from an arch bridge. Mech Syst Signal Process 2011;25(5):1431–50.
[2] Jaishi B, Ren WX, Zong ZH, Maskey PN. Dynamic and seismic performance of old multi-tiered temples in Nepal. Eng Struct 2003;25(14):1827–39.
[3] Bennati S, Nardini L, Salvatore W. Dynamic behaviour of a medieval masonry bell tower. II. Measurement and modelling of the tower motion. J Struct Eng ASCE 2005;131(11):1656–64.
[4] Ivorra S, Pallares FJ. Dynamic investigation on a masonry bell tower. Eng Struct 2006;25(5):660–7.
[5] Gentile C, Saisi A. Ambient vibration testing of historic masonry towers for structural identification and damage assessment. Constr Build Mater 2007;21(6):1311–21.
[6] Casarin F, Modena C. Seismic assessment of complex historical buildings: application to Reggio Emilia Cathedral, Italy. Int J Arch Heritage 2008;2(3):304–27.

[7] Pau A, Vestroni F. Vibration analysis and dynamic characterization of the Colosseum. Struct Control Health 2008;15(8):1105–21.
[8] Peña F, Lourenço PB, Mendes N, Oliveira DV. Numerical models for the seismic assessment of an old masonry tower. Eng Struct 2010;32(5):1466–78.
[9] Ramos LF, Marques L, Lourenço PB, DeRoeck G, Campos-Costa A, Roque J. Monitoring historical masonry structures with operational modal analysis: two case studies. Mech Syst Signal Process 2010;24(5):1291–305.
[10] Aras F, Krstevska L, Altay G, Tashkov L. Experimental and numerical modal analyses of a historical masonry palace. Constr Build Mater 2011;25(1):81–91.
[11] Oliveira CS, Çakti E, Stengel D, Branco M. Minaret behaviour under earthquake loading: the case of historical Istanbul. Earthquake Eng Struct D 2012;41:19–39.
[12] Gentile C, Saisi A. Operational modal testing of historic structures at different levels of excitation. Constr Build Mater 2013;48:1273–85.
[13] Cabboi A, Gentile C, Saisi A. Frequency tracking and FE model identification of a masonry tower. In: Proc. of the 5th Int. Operational Modal Analysis Conf., IOMAC'13, Guimaraes. Portugal; 2013.
[14] Cantieni R. One-year monitoring of a historic bell tower. In: Proc. of the 9th Int. Conf. on Structural Dynamics, EURODYN 2014. Porto, Portugal; 2014, p. 1493–00.
[15] Sánchez-Aparicio LJ, Riveiro B, González-Aguilera D, Ramos LF. The combination of geomatic approaches and operational modal analysis to improve calibration of finite element models: a case of study in Saint Torcato Church (Guimarães, Portugal). Constr Build Mater 2014;70:118–29.
[16] Gentile C, Saisi A, Cabboi A. Structural identification of a masonry tower based on operational modal analysis. Int J Arch Heritage 2015;9(2):98–110.
[17] Zuccoli N. Historic research on the Gabbia Tower (in Italian). Municipality of Mantua Internal Report; 1988.
[18] Saisi A, Gentile C. Post-earthquake diagnostic investigation of a historic masonry tower. J Cult Heritage; 2014. <http://dx.doi.org/10.1016/j.culher.2014.09.002>.
[19] Peeters B, De Roeck G. Reference-based stochastic subspace identification for output-only modal analysis. Mech Syst Signal Process 1999;13(6):855–78.
[20] Peeters B. System identification and damage detection in civil engineering [Ph.D. Thesis]. Katholieke Universiteit Leuven; 2000.
[21] SVS, ARTeMIS Extractor 2011. <http://www.svibs.com/>; 2012.
[22] Cantieni R. Experimental methods used in system identification of civil engineering structures. In: Proc. of the 1st Int. Operational Modal Analysis Conf., IOMAC'05, Copenaghen. Denmark; 2005. p. 249–60.
[23] Busatta F. Dynamic monitoring and automated modal analysis of large structures: methodological aspects and application to a historic iron bridge [Ph.D. Thesis]. Politecnico di Milano; 2012.
[24] Cabboi A. Automatic operational modal analysis: challenges and application to historic structures and infrastructures [Ph.D. Thesis]. University of Cagliari; 2013.
[25] Reynders E, Houbrechts J, De Roeck G. Fully automated (operational) modal analysis. Mech Syst Signal Process 2012;29:228–50.
[26] Brincker R, Zhang LM, Andersen P. Modal identification from ambient responses using Frequency Domain Decomposition. In: Proc. of the 18th Int. Modal Analysis Conf., IMAC-XVIII. San Antonio, USA; 2000. p. 625–30.
[27] Kvalseth TO. Cautionary note about R^2. Am Stat 1985;39:279–85.